

Implementation of an Exponential Mathematical Model of Power-Torque Curves in an Algorithm for Natural Aspirated and Turbocharged Internal Combustion Engines

GUSTAVO RUBEN DI RADO
Laboratorio de Simulación de Tránsito,
Universidad Nacional del Nordeste,
Av. Las Heras 727,
ARGENTINA

DANIEL SERGIO PRESTA GARCÍA
Laboratório de Sistemas de Transportes (LASTRAN),
Universidade Federal do Rio Grande do Sul,
Av. Osvaldo Aranha 99 sala 408/5,
BRASIL

Abstract: - Overtaking is one of the most complex maneuvers performed on two-lane rural highways, and its associated accidents account for a large proportion of the mortality connected to traffic accidents. In addition, the number of long vehicles, such as trucks or buses, using these traffic routes is increasing significantly. On the other hand, to perform this maneuver characterized by a fast and a slow vehicle, the engine of the fast one must have sufficient elasticity to achieve the required acceleration in the high gears, and in this sense, the turbo engine can provide this performance, with small engines and fuel savings. In this work, we develop an algorithm to simulate both naturally aspirated and turbocharged engines, fitting their characteristics based on an exponential model and comparing them with those on test benches.

Key-Words: - Driving Simulator, mathematical model, Power, Torque

Received: January 27, 2023. Revised: April 19, 2023. Accepted: May 15, 2023. Published: July 6, 2023.

1 Introduction

Two factors limit the performance of movement of a land vehicle on a flat surface from a standing position, [1]. The first is the maximum traction force exerted at the tire-road interface. That is, it forms at the contact surface mechanical and chemical bonds between the rubber that makes up the tires and the asphalt or the concrete that makes up a paved rolling surface. In not paved rolling surface, we can mainly determine traction by the mechanical forces exerted between the particles or roughness of the ground and the deformation of the tread.

The other influencing factor is the traction force that the engine can exert by transmitting torque to the clutch and, through a gear ratio, to the wheels. The lower of these two forces ultimately determines the potential acceleration of the vehicle.

In low gears, the slope and the rolling resistance limit the tractive force, i.e., the nature of the road and tire characteristics.

In high gears, on the other hand, where the influence of the wind and the slope of the terrain

counteract the movement, the tractive force is limited by the power-torque capacity of the engine and the type of transmission used.

In mountain roads with small radii horizontal curves, combined with vertical ones and built with only two lanes in opposite directions, the maneuver of overtaking becomes complex and dangerous, [20]. In these cases, in a situation of a climb, the heavy vehicles (HV), i.e., cargo vehicles for merchandise or people, also called slow-moving vehicles (SMV), considerably decrease their travel speed and, due to the reduced spaces to implement a safe overtaking maneuver, multiplies the risk. The performance of passenger cars or fast-moving vehicles (FMV) is crucial. The greater the acceleration capacity, i.e., the greater the elasticity of the engine, the faster an overtaking maneuver since less space is required and the time that the vehicle in question remains in the oncoming lane is less.

For nearly 25 years, driving simulators have been used in vehicle development research, driver

training (trains, airplanes, military vehicles, and more recently in trucks and cars), and also in studies of driver behavior on the road, [14].

Several reasons justify the use of driving simulators in traffic studies: Changes in the geometric design of roads, [21], studies in safety and signaling devices that do not yet exist and are expensive to build, test and study the behavior of drivers and pedestrians, [2], verification of the geometric consistency of projected or existing sections, [17], visibility in vertical and horizontal curves, [18] and, among the most important, is the simulation of the overtaking maneuver, [19].

These elements require a database of virtual vehicles of varying performance that faithfully represent real-world dynamic conditions regarding acceleration, terminal velocity, braking, maneuverability, and similar factors.

Low-displacement engines are becoming more common in the market due to their lower fuel consumption and CO₂ emissions. However, they have the disadvantage of slower acceleration, which makes overtaking difficult, especially on mountain roads. For this reason, turbocharged units power them.

This work aims to model mathematically the torque curves precisely for each internal combustion engine (ICE) analyzed, in this case, of two small displacement engines used in the market, and implement them in the SICOV (Simulador de COnducción de Vehículos) driving simulator, which we detail in section 3.1.

Another general representation proposed in [1] and [15] is based on a polynomial equation for modeling the power curve and, from this, obtains the torque curve, but the values obtained in it are far from the precision required for the objectives of this project, as shown in [13].

The main benefit of this study is to calibrate virtually the physical dynamics of the vehicles just mentioned, to obtain results that are closer to reality in driving simulation experiment projects.

2 Problem Formulation

Game engines provide a conducive environment for the development of driving simulators. Due to their built-in physics, they allow the adjustment of elements that affect vehicle dynamics. In this context, this article aims to integrate a collection of previous studies, [8], [9], [10], to provide calibrations to vehicles simulated in SICOV that make their dynamic behavior closer to that observed in real ones.

There are two typical curves to describe the characteristics and performance of an ICE. One is the full-load torque curve (accelerator pedal position at 100%), and the other is the corresponding power curve at full load (characteristic engine curve). Both are plotted against engine speed (usually in revolutions per minute RPM). On the other hand, the maximum braking force torque curve is plotted (0% of accelerator pedal position), which increases almost linearly with engine speed to a maximum of about 30% of rated torque, [3].

This work essentially consists of the simulation of this type of ICEs based on the principle of spark ignition and diesel. These kinds of engines maintain their dominant position in automotive engineering nowadays.

The main characteristics of spark ignition engines are a relatively high power-to-weight ratio, low fuel consumption, low cost, and easy starting, [4]. The disadvantages are the quality of fuel required and high consumption at low speeds.

These engines generate torque by igniting the fuel inside the cylinder. That is, as the size of the explosion inside the combustion chamber increases, the downward force on the piston also increases, thus increasing the torque produced by the engine. From here, it may seem logical that the higher the engine speed, the higher the torque value generated, but this is not the case.

The torque curve rises until it reaches a maximum value and then falls again compared to the steep rise of the power curve (Figure 1).

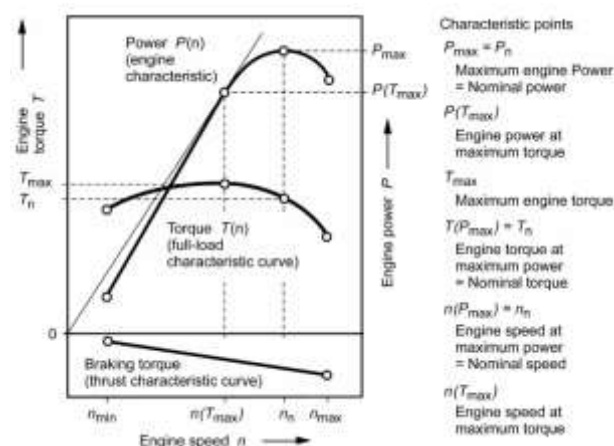


Fig. 1: Power – Torque curves of an internal combustion engine, [3]

One of the main reasons that the torque curve drops after its peak is the difficulty of forcing air into the engine.

Peak torque reaches a value where the mixing of fuel, air, and spark coincide to produce the highest

vertical force. As engine speed increases, however, it becomes difficult to obtain the air needed for combustion solely from the vacuum created by the piston descending after the exhaust stroke.

A device called a Control Unit Engine (CUE) is programmed to meet the torque requirement specified by the manufacturer. This device configuration aims to form a flat curve as much as possible for uniform distribution over the entire speed range.

2.1 Turbo vs Naturally Aspirated Engines

An internal combustion engine (ICE) requires fuel and air (oxygen) to produce mechanical power. The fuel injected into the cylinder depends on the amount of air administered, i.e., the fuel-to-air ratio (F/A). There is no point in injecting too much fuel if there is insufficient air because it will not burn due to the lack of oxygen, [5].

Depending on how the air draws into the cylinders, there are two main types of internal combustion engines:

- Naturally Aspirated Engines: In these engines, the air is drawn into the cylinders by the movement of the piston, which creates a vacuum as it moves toward the bottom dead center (BDC).

- Forced Induction (also known as supercharged): In this case, a compressor forces the air into the cylinders.

In naturally aspirated engines, the air pressure in the intake tract is always lower than the atmospheric pressure. It is 0.5 bar at idle and about 1 bar at full load with the throttle fully open.

For supercharged engines, the intake air pressure range (absolute) depends on the engine type:

- Gasoline engine (spark ignition): 0.5 bar at idle speed and 1.5 - 2.5 bar at full load.

- Diesel engine (compression ignition): 1.0 bar at idle speed and 2.5 bar at full load.

Supercharged engines divide themselves into two groups:

- Turbochargers: the compressor and the turbine connects mechanically to each other. The turbine is set in motion by the exhaust gas flow. There is no direct connection between the compressor and the crankshaft; the turbocharger and the engine link thermomechanically to each other.

- Mechanically Driven Superchargers: The crankshaft drives the supercharger; the supercharger and the engine have a direct (mechanical) connection, [5].

In both cases, the intercooler cools the air.

A significant advantage of supercharging is that air is introduced at high pressure, allowing more air inside and a complete fuel burnt, increasing the

power and resulting in a better elasticity of the engine.

Another significant advantage is that it is independent of the atmospheric conditions of the environment in which it circulates, especially in diesel engines, [4].

2.2 Vehicles Analyzed in the Simulation

For modeling and implementation purposes in the SICOV driving simulator, we selected two cars with low-displacement engines (1000 cm³). A naturally aspirated engine equips one of the cars and a turbocharged engine driven by exhaust gasses the other.

Figure 3 and Figure 5 show acceleration performance and top speed, while Figure 2 and Figure 4 show the characteristics of power–torque curves for the analysis.

Opel Corsa 1.0 EDI Turbo Eco FLEX 2017, [6]:

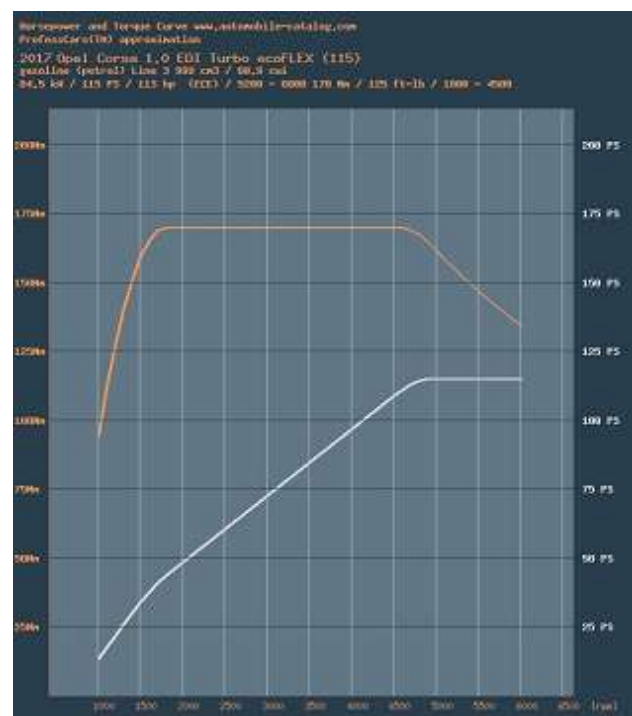


Fig. 2: Power – Torque curve Opel Corsa 1.0, [6]

- GM B10XFT engine (GM SGE Small Gasoline Engine series).
- Direct fuel injection
- Turbocharger
- 84.5 kW / 115 PS / 113 hp (ECE)/ 5200 - 6000.
- 170 Nm / 125 ft-lb/ 1800 - 4500.
- Gear ratio: I 3.917 (15.18), II 2.292 (8.88), III 1.556 (6.03), IV 1.167 (4.52), V 0.93 (3.6), VI 0.759 (2.94), final drive ratio 3.875, reverse ratio 3.833.
- Front-wheel drive
- Frontal area: 2.13 m²

- Estimated CX: 0.3
- Top speed: 198 km/h

- 107 Nm / 79 ft-lb/ 3250

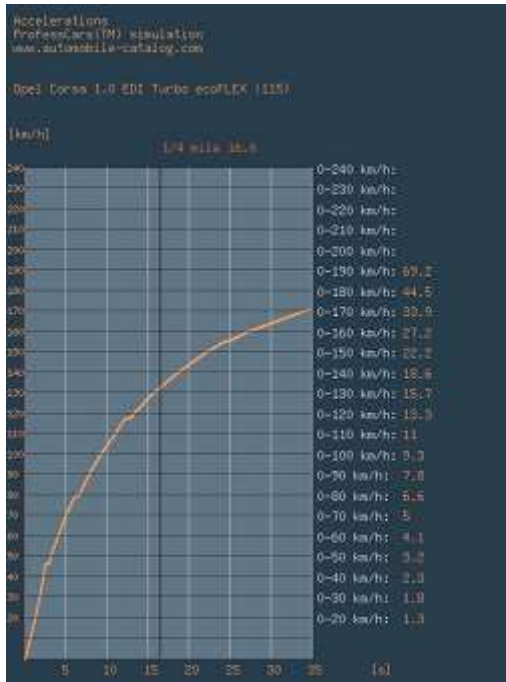


Fig. 3: Acceleration performance Opel Corsa 1.0, [6]

Fiat Uno Way 1.0 Flex (ethanol) 2020, [7]:

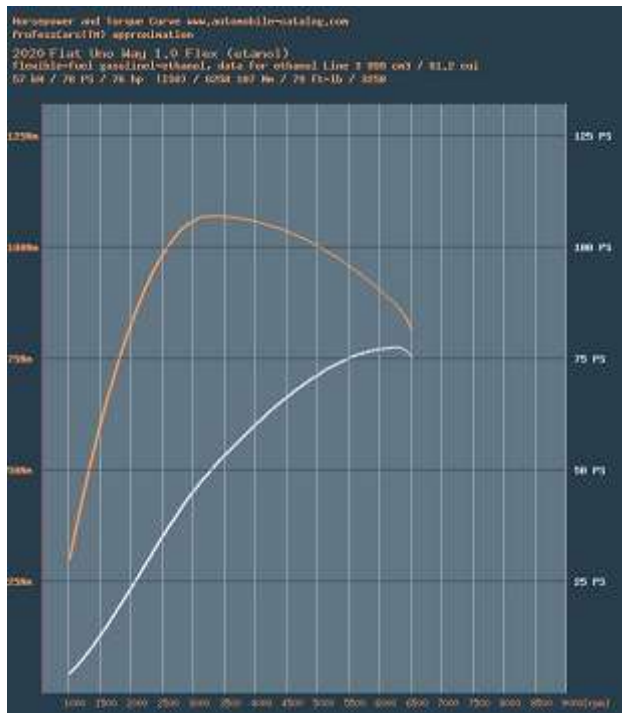


Fig. 4: Power – Fiat UNO Way 1.0, [7]

- Fiat Firefly Series Engine
- Direct injection
- Naturally Aspirated Engine
- 57 kW / 78 PS / 76 hp (ISO)/ 6250

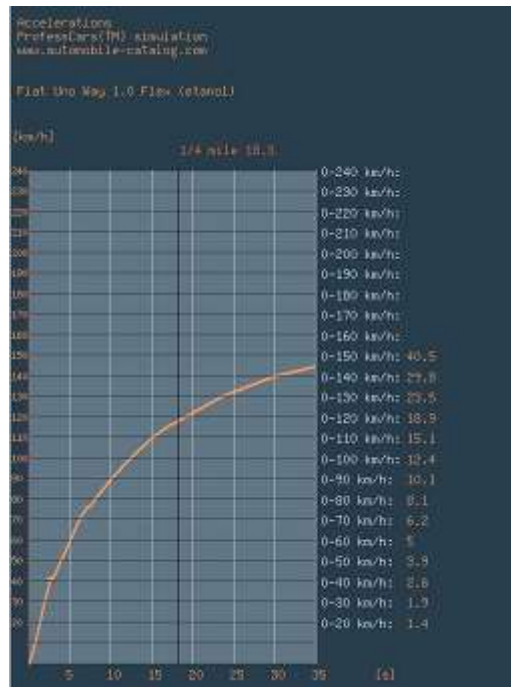


Fig. 5: Acceleration performance Fiat UNO Way 1.0, [7]

- Gear ratio: I 4.273 (17.38), II 2.316 (9.42), III 1.52 (6.18), IV 1.156 (4.7), V 0.838 (3.41), final drive ratio 4.067, reverse ratio 3.909.

- Front-wheel drive
- Frontal area: 2.13 m²
- Estimated CX: 0.3
- Top speed: 160 km/h

3 Problem Solution

3.1 SICOV Driving Simulator

The SICOV driving simulator is an academic project conducted for ten years by the Universidad Nacional del Nordeste (UNNE) of Argentina and the Universidade Federal do Rio Grande do Sul (UFRGS) of Brazil. It consists in developing a low-cost driving simulator through free gaming platforms such as UNITY®. The main interest is to achieve accurate vehicle dynamic simulation through the use of proven mathematical models and algorithms, [8], [9], [10], and the construction of virtual reality environments through the use of specific road construction software such as SAEPRO® (UFRGS) and 3D modeling software such as BLENDER®, [11].

The entire vehicle dynamic model of the SICOV driving simulator is being developed and coded in language c# at UNNE University, and the virtual

environment and road construction at UFRGS University. The equipment of the driving simulator consists of a Logitech® Driving Force sensitive racing wheel and pedals, as well as a Logitech® Driving Force shifter for manual gearing. Drivers can carry out the conduction with automatic transmission and paddles as well. The software enables using up to eight monitors to see the environment, building a complete vision around it. Additionally, it allows for an immersive experience through virtual reality headsets [16], as shown in Figure 6. Furthermore, it facilitates the use of different types of vehicles that users can drive, as well as AI cars.



Fig. 6: Driving simulator (left) – virtual scenario (right), [11]

The main goal is to obtain a computational tool for road design studies in terms of geometry and traffic movement, with an eye put on road safety, [12].

3.2 Mathematical Model Implemented

The torque curve of a naturally aspirated internal combustion engine (ICE) can be modeled with a good approximation by a quadratic equation and an exponential equation, dividing the model into four periods by different ranges of engine speed, [13], taking into account reference values such as maximum torque and nominal speed, i.e., the value of torque at which generates the highest engine power.

To create a general model suitable for representing torque curves for both naturally aspirated and turbocharged gasoline and diesel engines with sustained torque, a division of the algorithm into four periods is considered:

- For engine speeds below the maximum torque ($n < n(T_{max})$), the model that responds to the quadratic equation is used:

$$T(n) = T_{max} - \frac{T_{max} \cdot [n - n(T_{max})]^2}{[ci \cdot n(T_{max})]^2} \quad (1)$$

Where the coefficient ci , regulates the initial opening of the torque curve to simulate engines with more or less torque delivery at low revs.

- In turbo engines, there is a range of engine speeds in which maximum torque is maintained, i.e., in this interval ($n(T_{max}) < n < n_{turbo}(T_{max})$)

$$T(n) = T_{max} \quad (2)$$

- For engine speeds between the end of torque holding and the maximum rotational speed ($n_{turbo}(T_{max}) < n < n_{max}$):

$$T(n) = \left\{ \frac{T_n - T_{max}}{[cf_i \cdot (n_n - n(T_{max}))]^{cfe_i}} \cdot [n - n(T_{max})]^{cfe_i} + T_{max} \right\} \quad (3)$$

Where T_n is the nominal torque,

$$T_n = \frac{P_{max}}{\omega_n} \quad (4)$$

Equation (3) is bipartite as follows: from $n(T_{max})$ to n_n we use the modeling coefficients cf_1 and cfe_1 , and from n_n to n_{max} , we use the modeling coefficients cf_2 and cfe_2 . This process enables checking the degree of the curve in different ranges to fit precisely the characteristic values.

We explained all other variables in Figure 1.

Finally, the power is:

$$P(n) = T(n) \cdot n \quad (5)$$

3.2.1 Functionality of Coefficients

Calibration of the coefficients is essential to perform curve modeling. Their functions are as follows:

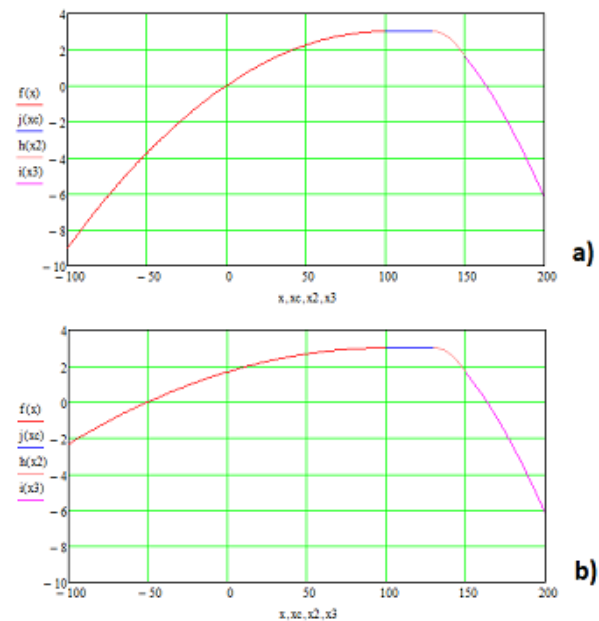


Fig. 7: ci modeling in the torque curve

Coefficient c_i models the initial part of the torque curve. It modifies the aperture between the idling speed and the engine speed at which maximum torque takes place, as Figure 7 shows as an example. In Figure 7a) $c_i = 1$, and in Figure 7b) $c_i = 1.5$.

It is crucial because, at this range, we find the torque delivery to the driving wheels at take-off from the rest moment, determining the start-up capacities of the simulated vehicle.

Coefficients c_{fi} and c_{fe_i} work together to determine the endpoint and the shape of the curve sections between the engine speed of maximum torque and the maximum engine speed, passing through the engine speed at the highest power, as Figure 8 shows as an example.

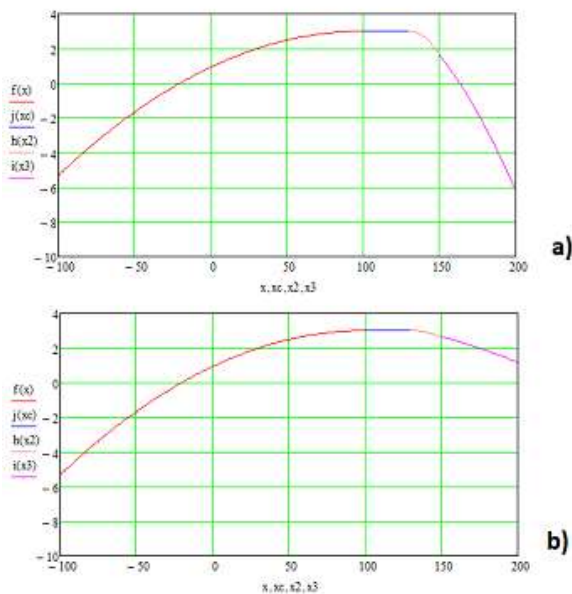


Fig. 8: c_{fi} and c_{fe_i} modeling in the torque curve

In Figure 8 a), $c_{fi} = 1$, $c_{fe_1} = 1.9$, $c_{f_2} = 0.8$ and $c_{fe_2} = 1.5$ and in Figure 8 b), $c_{fi} = 0.8$, $c_{fe_1} = 2.5$, $c_{f_2} = 2.2$ and $c_{fe_2} = 1.3$.

This process allows to model the torque delivery to the driving wheels from the highest engine speeds to the end of the curve.

3.3 Results of the Simulation

Figure 9 shows the characteristics curves of torque of the analyzed engines obtained from the simulation. The procedure was to leave the driving simulator in neutral gear and accelerate up to the maximum engine speed.

A comparison with the curves in Figure 2 and Figure 4 shows that the values match alongside a good approximation in all engine speed ranges.

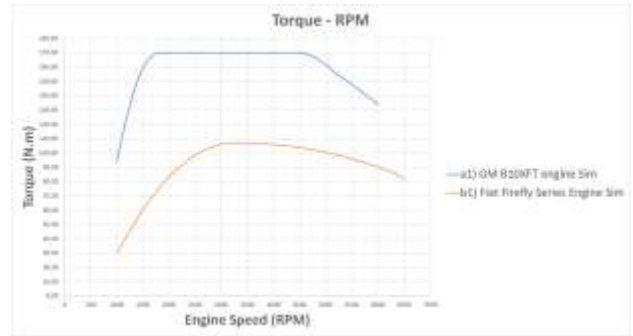


Fig. 9: Torque curves obtained from the simulation

Table 1 and Table 2 show the values at different engine speeds and a contrast between the general mathematical model proposed in this paper for the SICOV driving simulator and the curves determined in [6], [7].

Coefficient values for both engines in Eqs. (1) and (3) are as follows,

GM B10XFT engine (GM SGE Small Gasoline Engine series):
 $c_i = 0.665$, $c_{f_1} = 1$, $c_{fe_1} = 1.7$, $c_{f_2} = 1$, $c_{fe_2} = 1.17$

Fiat Firefly series engine:
 $c_i = 0.815$, $c_{f_1} = 1$, $c_{fe_1} = 2.1$, $c_{f_2} = 1.01$, $c_{fe_2} = 2.9$

Figure 10 shows the simplified flowchart of the simulation with the algorithm using the proposed mathematical model implemented. It also illustrates the inputs and outputs of the driving simulator.

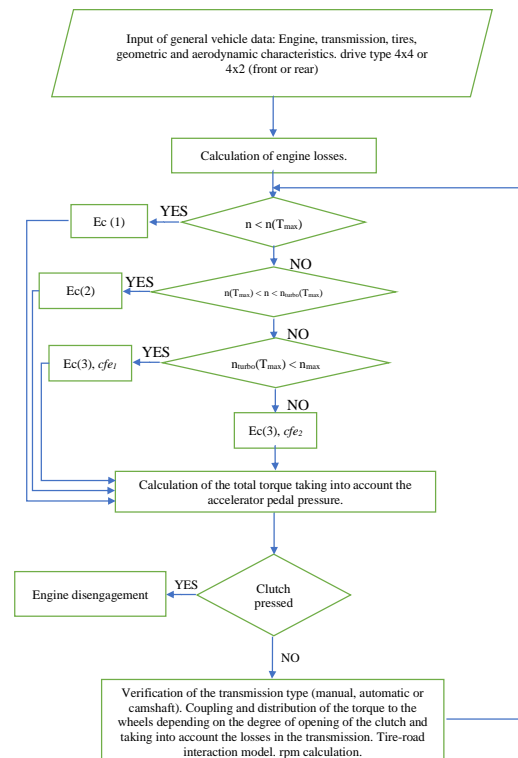


Fig. 10: Simplified flowchart

Table 1. Torque comparison GM B10XFT engine

GM B10XFT engine (GM SGE Small Gasoline Engine series).				
Math Model		[6]		
RPM	Torque	RPM	Torque	Error %
1000	94,07	1000	94,4	0,350
1100	111,86	1100	112,2	0,303
1200	127,29	1200	127,5	0,165
1300	140,34	1300	140,5	0,114
1400	151,02	1400	151,1	0,053
1500	159,32	1500	159,4	0,050
1600	165,25	1600	165,3	0,030
1700	168,81	1700	168,8	0,006
1800	170,00	1800	170	0,000
1900	170,00	1900	170	0,000
2000	170,00	2000	170	0,000
2200	170,00	2200	170	0,000
2400	170,00	2400	170	0,000
2500	170,00	2500	170	0,000
2600	170,00	2600	170	0,000
2700	170,00	2700	170	0,000
2800	170,00	2800	170	0,000
2900	170,00	2900	170	0,000
3000	170,00	3000	170	0,000
3100	170,00	3100	170	0,000
3200	170,00	3200	170	0,000
3300	170,00	3300	170	0,000
3500	170,00	3500	170	0,000
3600	170,00	3600	170	0,000
3700	170,00	3700	170	0,000
3800	170,00	3800	170	0,000
3900	170,00	3900	170	0,000
4000	170,00	4000	170	0,000
4100	170,00	4100	170	0,000
4200	170,00	4200	170	0,000
4300	170,00	4300	170	0,000
4400	170,00	4400	170	0,000
4500	170,00	4500	170	0,000
4600	169,46	4600	169,7	0,141
4700	168,24	4700	168,8	0,332
4800	166,49	4800	167,3	0,484
4900	164,27	4900	164,7	0,261
5000	161,63	5000	161,4	0,143
5100	158,59	5100	158,2	0,247
5200	155,18	5200	155,2	0,013
5300	152,67	5300	152,2	0,309
5400	150,11	5400	149,4	0,475
5500	147,50	5500	146,7	0,545
5600	144,84	5600	144,1	0,514
5700	142,15	5700	141,6	0,388
5800	139,41	5800	139,1	0,223
5900	136,64	5900	136,8	0,117
6000	133,84	6000	134,5	0,491
		Average		0,120

Table 2. Torque comparison Fiat Firefly Series Engine 1.0

Fiat Firefly Series Engine				
Math Model		[7]		
RPM	Torque	RPM	Torque	Error %
1000,00	29,79	1000	29,90	0,368
1100,00	36,50	1100	36,60	0,273
1200,00	42,91	1200	43,00	0,209
1300,00	49,01	1300	49,10	0,183
1400,00	54,80	1400	54,90	0,182
1500,00	60,29	1500	60,30	0,017
1600,00	65,48	1600	65,50	0,031
1700,00	70,36	1700	70,40	0,057
1800,00	74,93	1800	75,00	0,093
1900,00	79,20	1900	79,20	0,000
2000,00	83,17	2000	83,20	0,036
2100,00	86,83	2100	86,80	0,035
2200,00	90,19	2200	90,20	0,011
2300,00	93,24	2300	93,20	0,043
2400,00	95,98	2400	96,00	0,021
2500,00	98,42	2500	98,40	0,020
2600,00	100,56	2600	100,60	0,040
2700,00	102,39	2700	102,40	0,010
2800,00	103,91	2800	103,90	0,010
2900,00	105,13	2900	105,10	0,029
3000,00	106,05	3000	106,00	0,047
3100,00	106,66	3100	106,70	0,037
3200,00	106,96	3200	107,00	0,037
3250,00	107	3250	107,00	0,000
3300,00	107	3300	107,00	0,000
3400,00	107	3400	107,00	0,037
3500,00	106,9	3500	106,90	0,009
3600,00	106,8	3600	106,70	0,075
3700,00	106,6	3700	106,60	0,019
3800,00	106,4	3800	106,30	0,113
3900,00	106,2	3900	106,10	0,075
4000,00	105,9	4000	105,80	0,085
4100,00	105,6	4100	105,40	0,152
4200,00	105,2	4200	105,00	0,171
4300,00	104,8	4300	104,60	0,143
4400,00	104,3	4400	104,10	0,173
4500,00	103,8	4500	103,50	0,242
4600,00	103,2	4600	103,00	0,175
4700,00	102,6	4700	102,30	0,264
4800,00	101,9	4800	101,70	0,197
4900,00	101,2	4900	101,00	0,178
5000,00	100,4	5000	100,20	0,220
5100,00	99,6	5100	99,40	0,201
5200,00	98,74	5200	98,60	0,142
5300,00	97,83	5300	97,70	0,133
5400,00	96,86	5400	96,80	0,062
5500,00	95,85	5500	95,80	0,052
5600,00	94,78	5600	94,80	0,021
5700,00	93,66	5700	93,70	0,043
5800,00	92,49	5800	92,60	0,119
5900,00	91,27	5900	91,50	0,251
6000,00	90	6000	90,30	0,332
6100,00	88,67	6100	89,00	0,371
6200,00	87,3	6200	87,70	0,456
6300,00	86,2	6300	86,30	0,116
6400,00	84,16	6400	84,30	0,166
6500,00	81,99	6500	81,60	0,478
		Average		0,124



Fig. 11: SICOV simulator view with VR headset on

Figure 11 shows the modeled virtual reality scenario in which the tests were performed and the internal view of the Fiat UNO Way with the virtual reality headset attached.

3.4 Discussion of the Results

Figure 12 presents the overlapping curves derived from the mathematical model and those determined in [6], [7]. We obtain the relative error shown in Table 1 and Table 2 between these curves using Equation (6).

$$Err = \frac{|Torque\ Math\ Model - Measured\ Torque|}{Measured\ Torque} \quad (6)$$

Analyzing the situation for the GM B10XFT engine, it can be observed from Table 1 and curves a1) and a2) in Figure 12 that between an engine speed of 1000 RPM and 1700 RPM at the beginning of the sustained torque, the mean error is 0.134%. The curves match so well, indicating that, in this range, the quadratic model and the initial coefficient $c_i = 0.67$ fits the curve with precision.

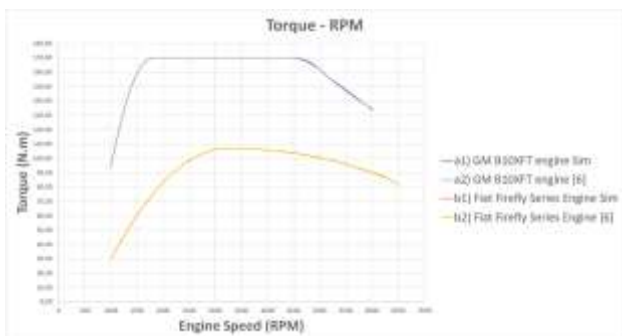


Fig. 12: Overlapping torque curves

Between the engine speed of 4600 RPM, at the end of the sustained torque, and 6000 RPM, the mean error is 0.312%, around three times higher than the mean of the first range of 0.134%. Despite this, the exponential coefficients cfe_1 and cfe_2 , with values of 1.7 and 1.17, making the curve slightly non-linear, match the curves acceptably well for the proposed objectives.

In the range of 1800 RPM to 4500 RPM, the torque is fixed at the maximum by the algorithm, resulting in zero error.

Considering the Fiat Firefly Series Engine 1.0, we can observe from Table 2 and curves b1) and b2) in Figure 12 that from 1000 RPM to 6200 RPM, the coincidence between the measured curve and the simulated one is very close, with a mean error of 0.117%. From 6300 RPM to 6500 RPM, the mean error is 0.253%, almost double. We can explain this because at 6250 RPM, the power curve reaches the maximum value, and from this point, the measured torque curve shows a slight deviation, making it hard to model. We could approximate this by giving the values of 1.01 to c_{f2} and 2.9 to c_{fe2} .

The mean error over the entire engine speed range for the GM B10XFT engine is 0.120%, and for the Fiat Firefly Series Engine 1.0, it is 0.124%.

4 Conclusion

The characteristic curve of the torque-speed diagram is crucial for determining the operation of car engines, and its mathematical modeling for use in driving simulators must be accurate, easy to implement, and general for all types of internal combustion engines (ICE). In the model proposed, the torque curve can be directly and easily fitted with the required accuracy by calibrating five coefficients, considering the experimental curves obtained by specialized workshops. As an essential part of the paper, we tested two engines with different operating modes (naturally aspirated and turbocharged) and manufacturers with good results. The modeled curves fitted the curves cataloged in [6], [7], with acceptable accuracy and low error.

From the comparison, we can conclude that the proposed mathematical model efficiently meets the requirements for developing a driving simulator aimed at road design studies.

As a main limitation of this study, we can mention that we can only use the proposed mathematical model in ICE. In future works, it will be necessary to study the shape and compound of the torque curves of hybrid and electric motors to model and implement them in the driving simulator.

References:

- [1] Genta Giancarlo, *Motor Vehicle Dynamics Modeling and Simulation*, World Scientific, 2006.
- [2] Felipe Rabay Lucas, Luis Eduardo Abrantes Russo, Renata Sayuri Kawashima, Aurenice Da Cruz Figueira, Ana Paula C. Larocca,

- Felipe Issa Kabbach Jr., Use of Driving Simulators Applied to the Road Safety Project, *Uso De Simuladores De Direção Aplicado Ao Projeto De Segurança Viária*, *Boletim de Ciências Geodesicas*, 2013.
- [3] Harald Naunheimer, Bernd Bertsche, Joachim Ryborz, Wolfgang Novak, *Automotive Transmissions*, Springer, 2011.
- [4] Wong J. Y., *Theory of Ground Vehicles*, John Wiley and Sons, inc, 2001.
- [5] X-engineer.org, (02/18/2017), *x-engineer*, <https://x-engineer.org/turbocharging/>, last accessed 04/15/2023.
- [6] PROFESS Pawel Zal, (06/07/2023), *automobile catalog*, https://www.automobile-catalog.com/curve/2017/2530250/opel_corsa_1_0_edi_turbo_ecoflex_115.html#gsc.tab=0, last accessed 04/15/2023.
- [7] PROFESS Pawel Zal, (06/07/2023), *automobile catalog*, https://www.automobile-catalog.com/car/2020/2989190/fiat_uno_way_1_0_flex_etanol.html#gsc.tab=0, last accessed 04/05/2023.
- [8] Di Rado, G. R., *Development of an off-road car driving simulation tool for road analysis and road safety. Desarrollo de una herramienta de simulación de conducción de automóviles todo terreno para análisis de carreteras y seguridad vial (doctoral thesis)*, <https://repositorio.unne.edu.ar/handle/123456789/27681?show=full>, Universidad Nacional del Nordeste, 2016.
- [9] Di Rado, G. R., Devincenzi, G. H., & García, D. S. P. Numerical integration method Runge and Kutta 4 (rk4) of differential equation application to a longitudinal model simulation of land vehicle dynamics. Aplicación del método de integración numérica de ecuaciones diferenciales runge y kutta 4 (rk4) a un modelo de simulación longitudinal de dinámica vehicular terrestre. *Computational Mechanics*, Vol. XXX, 2011, pp. 2907–2927.
- [10] Di Rado, G. R., Garcia, D. S. P., Devincenzi, G. H., & Silvero, F. Traffic simulation model of a land passenger car on a curved trajectory. Modelo de simulación de tránsito de un vehículo de paseo terrestre en trayectoria curva. *Computational Mechanics*, Vol. XXXV, 2017, pp. 1111–1136.
- [11] Andriola, C. L., *Behavioral validation of an immersive driving simulator. Validação comportamental de um simulador de direção imersivo (Master's Thesis)*, Universidade Federal do Rio Grande do Sul, 2021.
- [12] Kirsch Lanes, T., *Car following calibration model on a driving simulator. Calibração de modelo de car-following em simulador de direção (Master's Thesis)*, Universidade Federal do Rio Grande do Sul, 2023.
- [13] Di Rado, G. R., Presta García D. S., Application and Comparison of Mathematical Models of Aspirated Internal Combustion Engines in a Driving Simulator. Aplicación y Comparación de Modelos Matemáticos de Impulsores de Combustión Interna Aspirados en un Simulador de Conducción, *Computational Mechanics*, Vol. XXXVIII, 2021, pp.1091-1102.
- [14] Allen, Richard & Rosenthal, Theodore & Cook, M.L., A short history of driving simulation, *Handbook of Driving Simulation for Engineering, Medicine and Psychology*, 2011.
- [15] Jazar Reza N., *Vehicle Dynamics: Theory and Applications*, Springer, 2008.
- [16] Hurter J., Maraj C., Murphy S., Commercial virtual reality displays: Issues of performance and simulator sickness from exocentric depth-perception tasks, *Science Direct, Displays*, 2021.
- [17] Bobermin M., Silva M., Ferreira S., Driving simulators to evaluate road geometric design effects on driver behaviour: A systematic review, *Science Direct, Accident Analysis & Prevention*, 2023.
- [18] Mollu K., Biesbrouck M., Broeckoven L., Daniels S., Pirdavani A., Declercq K., Vanroelen G., Brijs K., Brijs T., Priority rule signalization under two visibility conditions: Driving simulator study on speed and lateral position, *Science Direct, Transportation Research Part F: Traffic Psychology and Behaviour*, 2018.
- [19] Figueira C., Larocca A., Analysis of the factors influencing overtaking in two-lane highways: A driving simulator study, *Science Direct, Transportation Research Part F: Traffic Psychology and Behaviour*, 2020.
- [20] Ritcher T., Ruhl S., Ortlepp J., Bakaba E., Causes, consequences and countermeasures of overtaking accidents on two-lane rural roads, *Science Direct, Transportation Research Procedia*, 2017.
- [21] Mussone L., Assessing the effects of road geometry and fidelity on driver behaviour in driving simulator experiments, *Science Direct, Transportation Research Interdisciplinary Perspectives*, 2023.

Contribution of Individual Authors to the Creation of a Scientific Article (Ghostwriting Policy)

Gustavo Ruben Di Rado carried out the development and optimization of the mathematical model.

Daniel Sergio Presta García contributed to the elaboration of the algorithm and simulation performance.

Sources of Funding for Research Presented in a Scientific Article or Scientific Article Itself

No funding was received for conducting this study.

Conflict of Interest

The authors have no conflict of interest to declare.

Creative Commons Attribution License 4.0 (Attribution 4.0 International, CC BY 4.0)

This article is published under the terms of the Creative Commons Attribution License 4.0

https://creativecommons.org/licenses/by/4.0/deed.en_US